*Proc. Natl. Acad. Sci. USA*
Vol. 79, pp. 4843–4847, August 1982
Biochemistry

# Electronic distributions within protein phenylalanine aromatic rings are reflected by the three-dimensional oxygen atom environments

(conformational stabilization/x-ray structure/thermodynamics/quantum mechanics)

KENNETH A. THOMAS*, GRAHAM M. SMITH*, THERESA B. THOMAS†, AND RICHARD J. FELDMANN‡

*Department of Biochemistry and Department of Scientific Information, Merck Institute for Therapeutic Research, Merck Sharp & Dohme Research Laboratories, Rahway, New Jersey 07065; †Information Systems Dept., Siemens Corp., Iselin, New Jersey 08830; and ‡Division of Computer Research and Technology, National Institutes of Health, Bethesda, Maryland 20014

*Communicated by P. Roy Vagelos, April 20, 1982*

ABSTRACT **The atomic environments of 170 phenylalanine-residue aromatic rings from 28 protein crystal structures are transformed into a common orientation and combined to calculate an average three-dimensional environment. The spatial distribution of atom types in this environment reveals a preferred interaction between oxygen atoms and the edge of the planar aromatic rings. From the difference in frequency of interaction of oxygen atoms with the edge and the top of the ring, an apparent net free energy difference of interaction favoring the edge of the ring is estimated to be about −1 kcal/mol (1 cal = 4.184 J). *Ab initio* quantum mechanical calculations, performed on a model consisting of benzene and formamide, indicate that the observed geometry is stabilized by a favorable enthalpic interaction. Although benzene rings are considered to be nonpolar, the electron distribution is a complex multipole with no net dipole moment. The observed interaction orientation frequencies demonstrate that these multipolar electron distributions, when occurring at the short distances encountered in densely packed protein molecules, are significant determinants of internal packing geometries.**

In the two decades since the elucidation of the myoglobin crystal structure, many interesting and useful generalizations about the structures of globular proteins have been made (1). One of the most important conclusions, based on time- and lattice-averaged x-ray crystallographic electron density maps, is that the interiors of proteins appear to be well ordered and efficiently packed (2).

Current understanding of the thermodynamics of folded protein structures is that the net stability of the native conformation is the small difference between large total stabilizing and destabilizing energies. The destabilizing entropic effect of ordering the flexible polypeptide chain is apparently overcome by an increase in randomness of the surrounding water upon removal of the nonpolar hydrophobic residues from solvent contact into the interior of the folded protein. It is usually assumed that the enthalpy of interaction of groups within the protein is comparable to the enthalpy of interaction of these protein groups with solvent. As a result of these considerations, protein folding is concluded to be driven by the increased entropy of the solvent (3–5).

Although the interactions encompassed in the enthalpy term may not lead to a net stabilization of a collapsed globular structure compared to a random coil, they can contribute to the stabilization of a unique packing order characteristic of the interior of each type of folded protein. This is clearly the case with buried charged or polar groups. Their transfer from the external highly polar aqueous environment into the lower-dielectric-constant hydrocarbon interior of proteins is facilitated by the interaction between buried groups of opposite charge or polarity (1). As a result of the constraint to pair these groups, they are expected to contribute to the high degree of order observed in the interior packing of proteins. Furthermore, this constraint should be enhanced by the degree to which the interactions, such as hydrogen bonding, are stabilized by specific relative orientations of the participating groups.

The similar order of the interior hydrophobic residues is less easily explained. In part, the potential disorder of the hydrocarbon side chains could be limited by the decreased conformational freedom left after optimization of charged and polar interactions. If directional forces involving nonpolar side chains are present, they could impose an additional constraint on the possible orientations of these side chains. We present the observation of energetically stable directional interactions involving the aromatic rings of phenylalanine residues and protein oxygen atoms.

## METHODS

**Protein Coordinates.** All protein atomic coordinates are taken from the data file of the Atlas of Macromolecular Structure on Microfiche (AMSOM) (6). Only structures with a nominal resolution greater than 2.5 Å are included. This gives a total of 28 proteins[§] containing 188 phenylalanine residues. Although only phenylalanine residues in unique subunits in oligomeric proteins are included in the environmental averaging, the full complement of subunits is generated so that the correct environments for the phenylalanine residues in the subunit contact regions are created. For phenylalanine residues that are at positions of sequence homology among multiple proteins, only one representative ring, from the highest resolution structure, is retained. In total, 18 residues are deleted based on sequence homology, leaving 170 residues with an average resolution of about 2.2 Å.

**Contact Environment.** The solvent-accessible surfaces of the ring atoms are determined in a manner similar to described methods (7–9). Protein environment atoms are considered to be in contact with the ring if $d_{e,r} \leq (r_e + r_r + 1)$, where $r_r$ and

The publication costs of this article were defrayed in part by page charge payment. This article must therefore be hereby marked "*advertisement*" in accordance with 18 U. S. C. §1734 solely to indicate this fact.

[§] The proteins included are: dogfish lactate dehydrogenase, human deoxyhemoglobin, liver alcohol dehydrogenase, concanavalin A, triose phosphate isomerase, prealbumin, lamprey hemoglobin, cytochrome $b_5$, tuna cytochrome *c*, bacterial cytochrome $c_2$, bacterial cytochrome $c_{550}$, sperm whale myoglobin, rubredoxin, high-potential iron protein, subtilisin, α-chymotrypsin, trypsin, elastase, thermolysin, carboxypeptidase A, bovine trypsin inhibitor, flavodoxin, ribonuclease A, staphylococcal nuclease, IgG $F(_{ab}')_2$ New, chicken lysozyme, carp parvalbumin, and carbonic anhydrase B.

$r_e$ are the individual radii of the ring and environmental atoms, respectively, and $d_{e,r}$ is the distance in Å between their centers. The distance requirement is relaxed by 1 Å because the x-ray coordinates have some error and the atoms in the closest shell of environmental atoms need not be in direct contact with the ring. Ring atoms and other atoms that are constrained by covalent bonding to be in close proximity to them, the $\alpha$- and $\beta$-carbons of the phenylalanine residue, and all of the atoms in the two adjacent peptide bonds, are deleted. About 25 environmental atoms remain in each phenyl contact environment.

**Environmental Averaging.** All phenylalanine rings and their contact environments are transformed into a common orientation. To enhance the statistical significance of environmental contacts, the symmetry of the ring is utilized to combine different portions of the environments. The ring and the $\beta$-carbon atom bonded directly to it have two mirror planes, one in the plane of the ring and one perpendicular to the ring plane passing through the $\beta$-, $\gamma$-, and $\zeta$-carbon atoms. Atoms in the environments are reflected through these two mirror planes so that they are all in the $(+X, \pm Y, +Z)$ sector. Utilization of the *mm* symmetry increases the contact density by a factor of four and enhances the reliability of the statistics of the distribution of atom types as a function of orientation about the ring.

The $(+X, \pm Y, +Z)$ space is divided into 15° toroidal sectors starting from the plane of the ring (0°) and progressing to the top of the ring (90°) (Fig. 1). The volume directly above the ring is formed by a cylinder of radius 1.38 Å (or a semicylinder after the symmetry combination operation). The distributions of atom types are examined in each of the toroidal sectors and the semicylinder. Because the volumes of equiangular toroidal sectors become smaller in progressing from the plane to the top of the ring, the atom-type frequencies are expressed as a percentage of total contacts. Because of the smaller number of atoms in the uppermost toroidal sector and the central cylinder, these two volumes are combined.

Results are expressed as the ratios of the number of oxygen atoms of a given type divided by the total number of atoms for each sector. These ratios are fit as a linear function of the angular distribution from the edge to the top of the ring by the method of least squares as weighted by the standard deviations of the ratios (10).

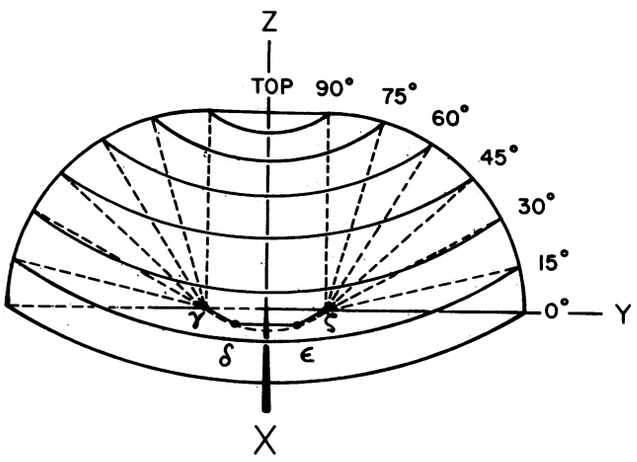


FIG. 1. Sectors used to partition the combined phenylalanine aromatic ring environments. A unique quadrant is shown after reduction by *mm* symmetry. Toroidal sectors divide the space from the edge (0°) to 90°. The "TOP" sector is a semicylinder directly above the half-ring. The axes and ring atoms are labeled. After the symmetry reduction, the $\delta_1$ and $\delta_2$ atoms and the $\varepsilon_1$ and $\varepsilon_2$ atoms each coincide and are labeled $\delta$ and $\varepsilon$, respectively.

**Quantum Mechanical Calculations.** *Ab initio* quantum mechanical calculations were performed with the Gaussian 80 program by using the 4-31G basis set (11). The zero interaction energy between molecules is taken as the sum of the individual molecular energies.

## RESULTS

**Observed Protein Phenylalanine Ring–Oxygen Atom Spatial Distribution.** The fraction of the total number of atoms that are oxygens in each of the toroidal sectors shown in Fig. 1 is given as a function of orientation from the side to the top of the phenylalanine aromatic ring in Fig. 2. The distribution reveals that the frequency of interactions of oxygen atoms with the phenyl ring is about 4 times greater at the edge than at the top of the aromatic ring.

The apparent free energy responsible for such a distribution can be calculated from $\Delta G_{app} = -RT \ln (N_B/N_A)$, where $\Delta G_{app}$ is the apparent free energy per interaction in cal/mol, $R$ is the gas constant (1.9872 cal deg.$^{-1}$ mol$^{-1}$), $T$ is the absolute temperature (298 K), $N_A$ is the fraction of oxygen atoms at the edge of the planar ring, and $N_B$ is the fraction at the top of the ring. In practice, $N_B$ and $N_A$ are taken to be the ratio values extrapolated to the edge and top of the ring from the weighted least squares line used to fit the distribution. The first $\Delta G_{app}$ value listed in Table 1 was derived from the distribution shown in Fig. 2. The analysis revealed that the interaction of an oxygen atom at the edge of a phenyl ring is more stable than at the top of the ring by a net energy of −0.8 kcal/mol.

From the water accessibility calculations, two-thirds of the phenylalanine rings have some degree of solvent exposure. To test the effect of solvent exposure, the distribution plots were calculated for the rings with totally defined contact environments ("buried") and those that have free regions that are large enough to accommodate a water molecule ("exposed"). The distribution energies are similar for completely determined internal versus partially determined external ring environments (Table 1). It also can be seen from the values in Table 1 that there is a somewhat greater energy difference for rings as a function of the secondary structure in which they occur.

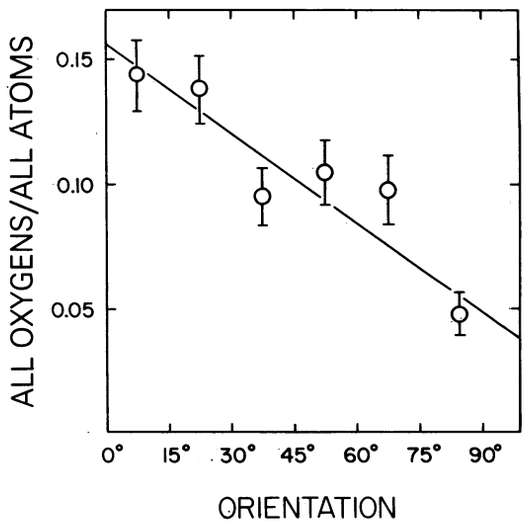


FIG. 2. Observed protein oxygen atom frequency as a function of orientation around the phenylalanine aromatic ring. Decimal fractions of atoms that are oxygens are shown as a function of angular sectors from the edge to the top of the ring. The uppermost toroidal sector and the adjacent semicylinder are combined. Error bars represent ± 1 $\sigma$. The straight line is the least-squares fit weighted by the standard deviations of individual ratios.

Table 1. Apparent free energies of interaction of subsets of phenylalanine aromatic ring environments and oxygen types*

| Phenyl environments | | Oxygen type | | $\Delta G_{app}$, kcal/mol |
|---|---|---|---|---|
| All | (170) | All | (458) | −0.8 |
| Internal | (55) | All | (140) | −0.9 |
| External | (115) | All | (318) | −0.8 |
| Helical | (55) | All | (112) | −0.9 |
| Beta | (64) | All | (196) | −1.2 |
| Coil | (51) | All | (150) | −0.5 |
| All | (170) | Noncarbonyl | (152) | −0.6 |
| All | (170) | Carbonyl | (306) | −0.9 |
| Internal | (55) | Carbonyl | (102) | −1.2 |
| External | (115) | Carbonyl | (204) | −0.9 |
| Helical | (55) | Carbonyl | (82) | −1.5 |
| Beta | (64) | Carbonyl | (132) | −1.1 |
| Coil | (51) | Carbonyl | (92) | −0.6 |

* Calculated from observed orientation distributions. The total number of phenylalanine rings and environmental oxygen atoms used to calculate the distributions are listed in parentheses for each subset.

Since two-thirds of the protein oxygen atoms are constituents of carbonyl groups, the distributions also were calculated for the carbonyl and noncarbonyl oxygen subsets. The apparent free energies derived from the distributions revealed that the oxygen atoms of the highly polar carbonyl group may form somewhat more stable complexes favoring the edge of the aromatic ring than do the noncarbonyl oxygen atoms (Table 1). Subdividing the ring distribution by the solvent exposure and secondary structure revealed energy values showing some quantitative differences among the subsets. Moreover, all types of categories fall within the range of $-1.0 \pm 0.5$ kcal/mol.

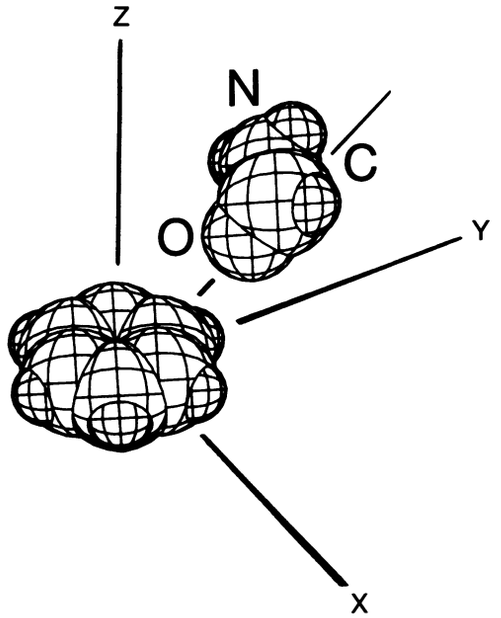


FIG. 3. Relative 45° orientation between the benzene and formamide molecules used for the calculation of the quantum mechanical energies. The formamide carbonyl carbon-to-oxygen vector, in the *Y-Z* plane, intersects the closest benzene carbon atom center. At the 0° orientation, the two molecules are coplanar in the *X-Y* plane. At increasing angles, the formamide plane is inclined to the benzene plane with no rotation of the formamide molecule about the carbonyl carbon-to-oxygen vector. At 90°, the carbon-to-oxygen vector intersects a benzene carbon atom center perpendicular to the benzene plane. At the TOP orientation the carbon-to-oxygen vector is coincident with the benzene 6-fold rotation axis (*Z* axis).

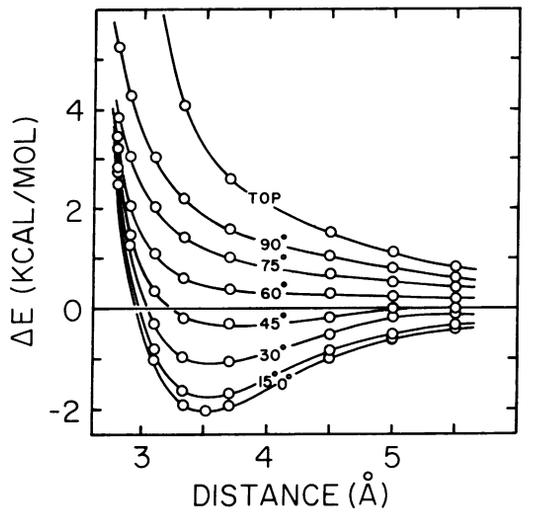


FIG. 4. Quantum mechanical interaction energy as a function of distance at a series of relative angular orientations. The net interaction energy between formamide and benzene, $\Delta E$, is given as a function of distance between the carbonyl oxygen atom and the ring carbon atom centers. Energy minima are observed at orientations from the edge of the benzene ring (0°) up to about 50°. At greater angles, the interaction is repulsive at all distances.

**Calculated Benzene–Formamide Energies.** As a result of various trials, the simplest adequate representation of the interaction between a peptide or amide carbonyl group found in proteins and the phenylalanine side chain was concluded to be formamide and benzene with the 4-31G basis set. Therefore, all quantum mechanical results utilized these molecules and this basis set. The energy of interaction of formamide and benzene was calculated as a function of orientation and distance between the two molecules. Starting with the two molecules coplanar with each other, the formamide–benzene carbon angle was increased at 15° increments to 90°. The 45° relative orientation

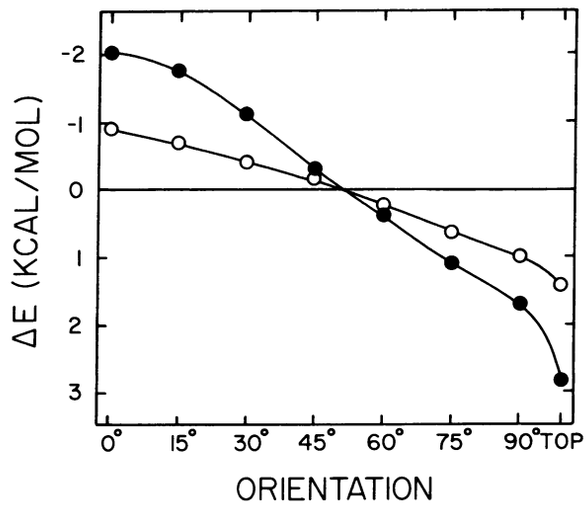


FIG. 5. Quantum mechanical interaction energy as a function of relative angular orientation at fixed distances. The net interaction energy between formamide and benzene, $\Delta E$, is given at an interatomic distance between the carbonyl oxygen and ring carbon atom centers of 3.6 Å (van der Waals contact; ●) and 4.6 Å (○), the largest atomic separation included in the observed distributions used to generate Fig. 2.

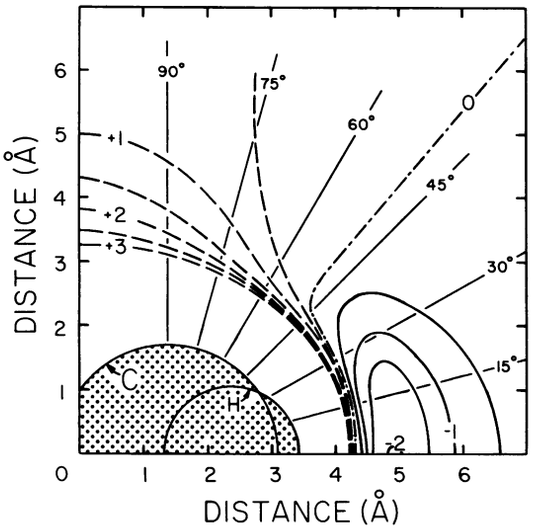


FIG. 6. Quantum mechanical isoenergy contours. The contours are plotted as a function of distance and orientation on a plane through the benzene ring formed by the 6-fold rotation axis along the ordinate and a benzene C—H bond along the abscissa. The value plotted at any point represents the energy of interaction, $\Delta E$, with the formamide carbonyl oxygen atom centered at that position. Contours plot repulsive (———), attractive (——), and zero (—·—·) energy and are drawn at 0.5 kcal/mol incremental values of $\Delta E$, with the integer values labeled. The van der Waals radii of the stippled benzene carbon and hydrogen atoms are labeled C and H, respectively. The angles corresponding to those in Fig. 1 are given.

is shown in Fig. 3. An additional orientation directly above the center of the ring was also calculated. The results of the calculations are shown in Fig. 4 in the common format of energy versus distance at a series of constant orientational angles. For comparison with the observed frequencies, the quantum mechanical interaction energies of benzene and formamide at two constant distances, the van der Waals sum and that value plus 1 Å, are given in Fig. 5 as a function of orientation angle. The greater distance is the maximum spacing included in the observed protein phenylalanine side chain–oxygen frequency calculations used to generate Fig. 2. The most revealing presentation of the data combines orientation and distance variables in a set of isoenergy contours (Fig. 6). This clearly represents the shape of the interaction energy surface around the benzene ring generated by its interaction with the formamide oxygen atom.

## DISCUSSION

The oxygen environments observed around the aromatic rings could be biased by local geometrical constraints. This might arise from either the local covalent bonding patterns or by conformational restrictions imposed by the hydrogen-bonded secondary structure. To insure that the oxygen distribution is not biased by the atoms held near the ring by covalent bonding patterns, the $\beta$- and $\alpha$-carbon atoms of the phenylalanine residue and the atoms in the adjacent peptide bonds are deleted from the atomic coordinates for the ring under consideration. Constraints imposed on the relative orientation of the aromatic ring and backbone oxygen atoms from nonadjacent peptide bonds are evaluated by subdividing the distributions as a function of the secondary structure in which the particular phenylalanine residue is located. The phenyl rings found in helical and beta structures have about the same or greater distribution energies than for the set of all rings. The rings found in coiled regions (i.e., those in neither helical nor beta structures) have the lowest distribution energies. The coiled backbone structures usually occur as external turns connecting segments of helical or $\beta$ structure. Although we cannot completely eliminate conformational biases against oxygen–ring edge interactions in this coiled subset, the dampened distribution differences for rings in these structures also may arise from uncertainties in the atomic environments. The uncertainties would be the result of both the often poorly determined protein conformation and the competition from the large but undefined water contribution at the loosely ordered and highly exposed external turns.

In fact, based on additional quantum mechanical calculations with benzene and water (data not presented), the energy of interaction, $\Delta E$, favors the oxygen approach to the edge of the ring and the interaction of the water hydrogen with the ring face. In both cases, the maximum energies of attraction are about −2.5 kcal/mol. Orientations with either the water oxygen directed toward the benzene face or the water hydrogen approaching the edge of the ring are repulsive. In an attempt to evaluate the effect of unidentified water molecules, the observed protein oxygen atom distributions were calculated for both those rings that are buried and have totally defined environments and those that have some undefined areas at which water can interact. In fact, most rings that have areas of solvent exposure are still largely buried. Therefore, it is not surprising that the energy differences, although slightly larger for the internal rings, are very similar. It appears that nothing is occurring in the undefined solvent region that significantly alters the orientation between the ring and the protein oxygen atoms.

It should be noted that the distribution energies are calculated for the rings in an environment of protein atoms. Therefore, the oxygen distribution energy is calculated in the presence of an average environment of other competing interactions. Additional quantum mechanical calculations (data not shown) have revealed, however, that there is no net energy of attraction between ethane and benzene with the ethane carbon-to-carbon vector coaxial to either the benzene 6-fold rotation axis or an aromatic C—H bond. Therefore, it is unlikely, barring other conformational constraints, that an aliphatic side chain can effectively compete with a protein oxygen atom to occupy a position at the edge of a phenylalanine aromatic ring. Nevertheless, other interactions that have not been evaluated may dampen the ring–oxygen atom orientational distribution differences. The energy calculated from the distributions, $\Delta G_{app}$, is then a residual, or apparent, free energy (i.e., the energy that is in excess over that needed to compete with other interactions). We already have mentioned water as a potential competitor of the carbonyl group for the ring hydrogen atoms. In addition, many of the oxygen atoms, especially those in secondary structures, are hydrogen bonded. Although this could be expected to weaken the interaction of the oxygen atoms with the edge of the aromatic rings, it would not eliminate the stable oxygen–ring interaction. As reviewed by Finney (12), hydrogen bond formation is not mutually exclusive with other electrostatic interactions of the constituent oxygen atoms. It is observed in protein structures that the carbonyl oxygens can interact simultaneously with two hydrogen-bond donors. This is interpreted to result from two lone pairs of electrons on each carbonyl oxygen. A backbone amide N—H, on the other hand, typically interacts with only one carbonyl oxygen (13). Therefore, in a hydrogen bond between a peptide N—H and carbonyl oxygen, the oxygen atom is available for additional electrostatic interactions.

As shown in Fig. 5, the energy differences between carbonyl oxygen interactions at the top and at the edge of the benzene ring, calculated from the quantum mechanical approach, varies from −2.5 kcal/mol at the greatest distance included in the

protein oxygen–phenyl carbon atom environment calculation ($r_e + r_r + 1$) to −5 kcal/mol at the distance equal to the sum of the van der Waals radii of these atoms ($r_e + r_r$). These values were determined with the carbon-to-oxygen dipole roughly perpendicular to the surface of the benzene ring. Based on the electron distribution within the benzene ring (see below) this orientation might be expected to generate one of the largest energy differences between the top and edge of the ring. However, many carbonyl dipoles probably intersect the aromatic ring surface at skew angles, and the resulting energy differences may be less. Rotation of the formamide around the carbon-to-oxygen vector axis has virtually no effect on the calculated energies. With the oxygen center held fixed, all other orientations of the formamide that were examined (data not presented) resulted in interaction energies that were no less than 50% of those given above.¶ We can relate these calculated energies to the enthalpic component of free energy derived from the observed orientation distributions by assuming that $\Delta E \cong \Delta H$ at the constant pressure and volume of the idealized quantum mechanical calculations.¶ Therefore, it can be inferred that a negative enthalpy of interaction between carbonyl oxygen atoms and the edge of phenyl rings contributes to the overall stability of these contacts in proteins.

These observations give a picture of benzene as favoring interactions of atoms with partial negative charges, such as oxygens, at the edge of the ring and disfavoring them at the ring faces. This is in qualitative agreement with a multipolar distribution for benzene with electron-rich faces and a ring of hydrogens, having a partial positive charge (as indicated by the C—H bond dipole moments) around the edge. This model can be used to anticipate other interactions with the aromatic ring. One such interaction is among rings seen in the molecular packing within benzene crystals. Here benzene molecules pack so that the edge of one ring is directed at the faces of adjacent rings (14). In other words, the positively charged edge interacts with the negatively charged faces. Such an arrangement also has been noted in the single example of a large phenylalanine side-chain cluster in proteins—that of carp parvalbumin (15). In this case, the packing, described as a "herringbone" pattern, shows the same edge-to-face orientations. Quantum mechanical calculations indicate that this type of interaction has a favorable energy of stabilization, whereas the face-to-face orientation is repulsive (unpublished observations).

These results demonstrate that elements of the immediate packing environments of phenylalanine side chains in proteins are determined by the free energy of interaction with a stabilizing contribution from the enthalpy of local interaction. In a broader sense, this shows that the specific geometry of packing of phenylalanine and perhaps other aromatic side chains is determined, at least in part, by the energies of interaction of the constituent hydrocarbon groups and not only by the requirements to efficiently pack these residues so as to maximize internal ionic and hydrogen bonding interactions. Because the net free energy favoring the folded state of proteins is estimated to be about −10 kcal/mol (16), the apparent free energy of an internal phenylalanine ring–oxygen atom interaction of about −1 kcal/mol can make a significant contribution to the overall stability of the folded conformation.

¶ The calculated quantum mechanical energies do not include the contribution from the London dispersion force. This energy term arises from a correlation, or resonance, of electron movement so that the instantaneous dipole moments that are created by the electron distributions on adjacent nonbonded atoms align to generate an attraction. Dispersion is usually considered to be a weak force that becomes significant when other normally stronger interactions are weak or absent (such as interactions between atoms of a noble gas). Currently, it is not feasible to calculate a reliable value for the dispersion force for a system with this large number of orbitals.

K.A.T. and T.B.T. thank Dr. Ralph Bradshaw (Washington University, St. Louis) and Dr. Alan Schechter (National Institutes of Health) for support during portions of this work. We also thank Dr. Lenard Banazak (Washington University, St. Louis) and the Seven-Up Co. for providing computing facilities. Finally, we are grateful to Dr. Bernhard Schlegel (Wayne State University) for advice on the use of the Gaussian 80 program.

1. Thomas, K. A. & Schechter, A. N. (1980) in *Biological Regulation and Development*, ed. Goldberger, R. F. (Plenum, New York), Vol. 2, pp. 43–100.
2. Richards, F. M. (1974) *J. Mol. Biol.* **82**, 1–14.
3. Kauzmann, W. (1959) *Adv. Protein Chem.* **14**, 1–63.
4. Tanford, C. (1968) *Adv. Protein Chem.* **23**, 121–282.
5. Tanford, C. (1970) *Adv. Protein Chem.* **24**, 1–95.
6. Feldmann, R. (1976) *AMSOM-Atlas of Macromolecular Structure on Microfiche* (Tracor-Jitco, Rockville, MD).
7. Lee, B. & Richards, F. M. (1971) *J. Mol. Biol.* **55**, 379–400.
8. Shrake, A. & Rupley, J. A. (1973) *J. Mol. Biol.* **79**, 351–371.
9. Finney, J. L. (1975) *J. Mol. Biol.* **96**, 721–732.
10. Bevington, P. R. (1969) *Data Reduction and Error Analysis for the Physical Sciences* (McGraw-Hill, New York).
11. Binkley, J. S., Whiteside, R. A., Krishan, R., Seeger, R., DeFrees, D. J., Schlegel, H. B., Topiol, S., Kahn, L. R. & Pople, J. A. (1980) *GAUSSIAN 80, An Ab Initio Molecular Orbital Program*, Quantum Chemistry Program Exchange (Indiana University, Bloomington, IN), Vol. 13, No. 406.
12. Finney, J. L. (1978) *J. Mol. Biol.* **119**, 415–441.
13. Kretsinger, R. H. & Nockolds, C. E. (1973) *J. Biol. Chem.* **248**, 3313–3326.
14. Wyckoff, R. W. G. (1969) *Crystal Structures* (Wiley, New York), 2nd Ed., Vol. 6, Part I, pp. 1–2.
15. Nockolds, C. E., Kretsinger, R. H., Coffee, C. J. & Bradshaw, R. A. (1972) *Proc. Natl. Acad. Sci. USA* **69**, 581–584.
16. Pace, C. N. (1975) *CRC Crit. Rev. Biochem.* **3**, 1–43.